Supramolecular Chemistry
Publication details, including instructions for authors and subscription information:
http://www.informaworld.com/smpp/title~content=t713649759

Kinetics of Desolvation of Related Organic Inclusion Compounds

M. R. Caira[a]; A. Coetzee[a]; L. R. Nassimbeni[a]; E. Weber[b]; A. Wierig[b]
[a] Department of Chemistry, University of Cape Town, Rondebosch, South Africa [b] Institut für Organische Chemie, Technische Universität Bergakademic Freiberg, Germany

To cite this Article Caira, M. R. , Coetzee, A. , Nassimbeni, L. R. , Weber, E. and Wierig, A.(1999) 'Kinetics of Desolvation of Related Organic Inclusion Compounds', Supramolecular Chemistry, 10: 4, 235 — 241
To link to this Article: DOI: 10.1080/10610279908054507
URL: http://dx.doi.org/10.1080/10610279908054507

SUPRAMOLECULAR CHEMISTRY, Vol. 10, pp. 235–241
Reprints available directly from the publisher
Photocopying permitted by license only

Published by license under
the Gordon and Breach Science
Publishers imprint.
Printed in Malaysia.

Kinetics of Desolvation of Related Organic Inclusion Compounds*

M. R. CAIRA[a], A. COETZEE[a,†], L. R. NASSIMBENI[a], E. WEBER[b] and A. WIERIG[b]

[a]*Department of Chemistry, University of Cape Town, Rondebosch, 7701, South Africa;*
[b]*Institut für Organische Chemie, Technische Universität Bergakademie Freiberg, Germany*

(Received 13 March 1998; In final form 26 October 1998)

This study dealt mainly with the structure-reactivity relationship of selected organic inclusion compounds. The crystal structures of the inclusion compounds of three related hosts, 2,2′-bis(2,7-di-*tert*-butyl-9-hydroxy-9-fluorenyl)biphenyl, 2,2′-bis(2,7-dichloro-9-hydroxy-9-fluorenyl)biphenyl and 2,2′-bis(2,7-dibromo-9-hydroxy-9-fluorenyl)biphenyl with 1,4-dioxane (Compound 1), 1,3-dioxane (Compound 2) and 1,3-dioxolane (Compound 3) respectively were elucidated, using single crystal X-ray crystallography. It was found that the guests were either located in channels or constricted channels (cavities), formed by the host framework. The kinetics of desolvation of these compounds were studied and their activation energies were compared.

Keywords: Inclusion compound, desolvation kinetics

INTRODUCTION

Molecules which contain the fluorene moiety have proved to be successful hosts, capable of forming inclusion compounds with a variety of guests [1]. These hosts are often functionalised by an hydroxyl group at position 9, and are sometimes dimerised *via* an aromatic moiety such as biphenyl, to yield a crowded diol host molecule [2]. A most versatile host compound of this kind is 2,2′-bis(9-hydroxy-9-fluorenyl)biphenyl, which enclathrates a large number of guests, including aliphatic alcohols, nitriles, amines, ketones and pyridines [3]. The crystal structures of this host with acetonitrile, cyclohexanone, di-*n*-propylamine and dimethylformamide were studied and it was noted that the rigidity of the host conformation was maintained, irrespective of the guest species [4]. Substituting the fluorene moieties at the 2 and 7 positions with bulky groups such as halogens, also yields successful host compounds, which are often stabilised by hydrogen bonds between host and guest [5]. The literature reveals very few studies in which attempts have been made to correlate the kinetics of decomposition reactions with crystal structures [6]. The structures of the inclusion compounds of 2,2′-bis(2,7-dichloro-9-hydroxy-9-fluorenyl)biphenyl with 1,4-dioxane and 1,3-dioxolane [7] were elucidated and their thermal desolvation studied. Attempts were made to relate the

---

*Complexation with Diol Host Compounds, Part. 27.
[†] Corresponding author. Fax: +27 21 689 7499.

structures and thermal desolvation of two related host compounds, 2, 2′-bis(2,7-dichloro-9-hydroxy-9-fluorenyl)biphenyl and 2,2′-bis(2,7-di-*tert*-butyl-9-hydroxy-9-fluorenyl)biphenyl, which form inclusion compounds with acetone [8].

In this paper we present the structural results and kinetics of desolvation of the inclusion compounds of three related hosts, 2,2′-bis(2,7-di-*tert*-butyl-9-hydroxy-9-fluorenyl)biphenyl, 2,2′-bis(2,7-dichloro-9-hydroxy-9-fluorenyl)biphenyl and 2,2′-bis(2,7-dibromo-9-hydroxy-9-fluorenyl) biphenyl with 1,4-dioxane (Compound **1**), 1,3-dioxane (Compound **2**) and 1,3-dioxolane (Compound **3**) respectively (see Scheme 1). The kinetics were analysed by isothermal decomposition runs at selected temperatures, and curve fitting techniques allowed us to select suitable models to describe the desolvation mechanism and derive the appropriate Arrhenius parameters.

EXPERIMENTAL

The inclusion compounds were obtained by dissolving the appropriate host compound [5] in an excess of the solvent to the included. Single crystals of diffraction quality were obtained by slow evaporation of these solutions in glass vials covered with perforated parafilm. Single crystals of suitable size (typically between 0.2 and 0.5 mm in all dimensions) were flame sealed in Lindemann capillary tubes together with mother liquor in order to prevent desorption of the guest. X-ray diffraction data were measured on an Enraf-Nonius CAD4 diffractometer, using graphite-monochromated MoK$_\alpha$ radiation, ($\lambda = 0.7107$ Å). Accurate cell parameters were determined from 24 reflections at θ 10–12°. The unit cell was refined by least-squares analysis of the setting angles of 24 reflections collected in the θ range 16–17° and centred on the diffractometer. Data

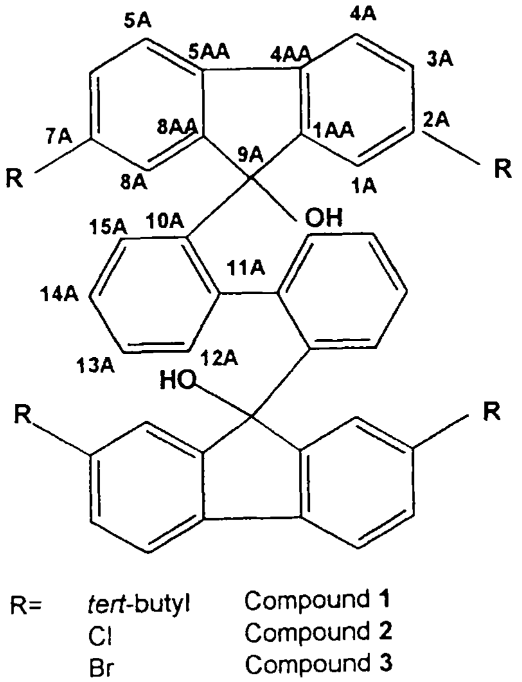

R=		
	tert-butyl	Compound **1**
	Cl	Compound **2**
	Br	Compound **3**

SCHEME 1 Numbering scheme.

were collected in the $\omega - 2\theta$ scan mode. The vertical aperture length was fixed at 4 mm, the aperture width at $(1.12 + 1.05 \tan\theta)$ mm and the scan width at $\omega = (x + 0.35 \tan\theta)^\circ$, with $x = 0.80$ or 0.85. During data collection three reference reflections were monitored periodically to check crystal stability. The data reduction included correction for Lorentz and polarisation effects. In the cases where heavy atoms (Cl, Br) were present in the host, an empirical absorption correction was applied [9]. Crystal data and structural refinement parameters are given in Table I.

Differential scanning calorimetry (DSC) and thermogravimetry (TG) were performed on a Perkin Elmer PC7 series system. Powdered specimens were blotted dry on filter paper and placed in open platinum pans for TG experiments and in crimped, but vented aluminium sample pans for DSC experiments. Sample weight in each case was 2 to 5 mg. The temperature range for the programmed temperature runs was 30–390°C, recorded at a heating rate of $20^\circ\mathrm{C\,min^{-1}}$. The samples were purged by a stream of nitrogen flowing at $40\,\mathrm{mL\,min^{-1}}$. Data for the isothermal kinetics of desolvation were obtained from TG experiments done at selected temperatures.

RESULTS AND DISCUSSION

Structure Solution and Refinement

The structures were solved by direct methods, using the program SHELX-86 [10] and refined

TABLE I

Code	1	2	3
Guest	1,4-dioxane	1,3-dioxane	1,3-dioxolane
Molecular formula	$C_{54}H_{58}O_2 \cdot C_4H_8O_2$	$C_{38}H_{22}O_2Cl_4 \cdot 2(C_4H_8O_2)$	$C_{38}H_{22}O_2Br_4 \cdot 2(C_3H_6O_2)$
$M_r/\mathrm{g\,mol^{-1}}$	915.21	828.56	978.35
Temperature/K	294(2)	294(2)	294(2)
Crystal data			
Crystal system	Monoclinic	Monoclinic	Monoclinic
Space group	C2/c	C2/c	C2/c
a/Å	17.217(5)	22.08(1)	21.570(8)
b/Å	17.895(3)	11.414(7)	11.717(3)
c/Å	17.219(3)	18.60(1)	18.37(1)
$\beta/^\circ$	113.18(2)	124.06(5)	124.22(4)
Z	4	4	4
V/Å^3	4877(2)	3883(4)	3840(4)
$D_c/\mathrm{g\,cm^{-3}}$	1.246	1.417	1.692
$\mu(\mathrm{MoK_\alpha})/\mathrm{cm^{-1}}$	0.78	3.56	42.42
F(000)	1976	1720	1944
Data collection			
Crystal dimensions/mm	0.28 × 0.28 × 0.28	0.37 × 0.34 × 0.34	0.34 × 0.21 × 0.21
Range scanned $\theta/^\circ$	1.72 to 24.98	2.10 to 24.99	2.08 to 24.97
Range of indices h, k, l	−20,18; 0,21; 0,20	−26,20; −13,0; −22,20	−25,21; 0,13; 0,21
No. of reflections collected	4457	3526	3493
No. of unique reflections	4300	3413	3376
No. of reflections observed with $I_{rel} > 2\sigma I_{rel}$	2025	1822	2084
Final refinement			
No. of restraints	2	0	2
No. of parameters	288	256	220
R1 ($I_{rel} > 2\sigma I_{rel}$)	0.0894	0.0809	0.0462
wR2 ($I_{rel} > 2\sigma I_{rel}$)	0.2596	0.2020	0.1210
Max. height in electron density map/e Å^{-3}	0.632	0.617	0.710
Min. height in electron density map/e Å^{-3}	−0.455	−0.493	−0.708

by full-matrix least-squares methods against F^2 using SHELXL-93 [11]. A weighting scheme (w) was refined for each structure, where:

$$w = 1/[\sigma^2(F_o^2) + (aP)^2 + bP]$$
$$P = [\max(0, F_o^2) + 2F_c^2]/3$$

and a and b were refined for each structure.

For Compound **1** direct methods yielded the positions of all the host non-hydrogen atoms in the asymmetric unit, except for the C atoms on the *tert*-butyl groups, which together with the non-hydrogen atoms in the guest molecule were located in the difference electron density maps upon subsequent refinement. Compound **1** crystallises in the space group C2/c with Z = 4. This requires the host molecule to be located on a diad at Wyckoff position *e*. Most of the host non-hydrogen atoms were refined anisotropically. High thermal motion was observed in the *tert*-butyl groups and only the pivotal C atoms [C(16A) and C(20A)] were refined anisotropically. The guest showed high thermal motion and was refined isotropically. The hydroxyl hydrogen atoms were located in the difference electron density maps and refined with bond length constraints and individual temperature factors. The rest of the hydrogen atoms were placed with geometric constraints and refined with a common isotropic temperature factor for similar groups. The host molecule is locked into conformation [with C(10A)-C(11A)-C(11A′)-C(10A′) = 90(1)°] *via* an intramolecular hydrogen bond [O(9A)···O(9A′) = 2.744(7) Å]. The host: guest ratio of 1 : 1 requires half a 1,4-dioxane molecule to be located in the asymmetric unit. The dioxane molecule was located on a centre of inversion, at Wyckoff position *a*. Careful analysis of the difference electron density map revealed that the guest molecule is in fact disordered. The dioxane molecule was modelled with two possible positions for the oxygen atom [O(2G) with a site occupancy of 0.70 and O(2GA), with a site occupancy of 0.30]. The site occupancy factors were based on the relative peak heights in the electron density map. An intermolecular hydrogen bond exists between the guest molecule and host with O(9A)-H(9A)···O(2G) = 2.81(1) Å. O(2GA) does not take part in any hydrogen bonding. The crystal packing, viewed down [001] is shown in Figure 1. The guests lie in constricted channels running parallel to [001].

The structures of Compounds **2** and **3** were solved in a similar manner. There are four host molecules in the unit cell (Z = 4), with the host molecule located in a special position, at Wyckoff position *e*. For Compound **2** all non-hydrogen atoms were refined anisotropically. The central biphenyl residue is twisted at right angles with the torsion angle C(10A)-C(11A)-C(11A′)-C(10A′) = 96.9(7)°. The host : guest ratio of 1 : 2 required the guest to be located in a general position. The structure is stabilised by a host to guest hydrogen bond, O(9A)-H(9A)···O(1G), with d(O···O) = 2.835(6) Å. The crystal packing diagram viewed down [010] of Compound **2** is shown in Figure 2.

Compound **3** is isostructural with Compound **2** and exhibits the same host packing motif. This is also similar to the structure reported for the 1 : 2 inclusion compound of 2,2′-bis(2,7-dichloro-9-hydroxy-9-fluorenyl)biphenyl with 1,3-dioxolane [12]. In these structures the host molecules stack along "wavy" layers parallel to [001] which constrict at (1/4, y, 1/2) so as to form channels running parallel to [010]. The guest

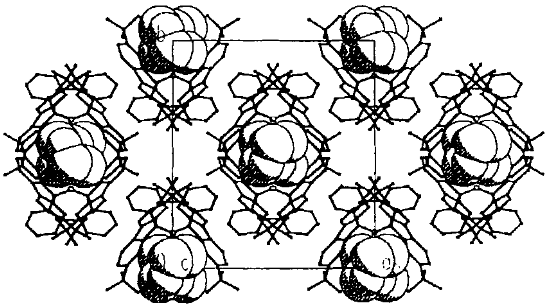

FIGURE 1 Projection of the crystal packing in Compound 1, viewed down [001].

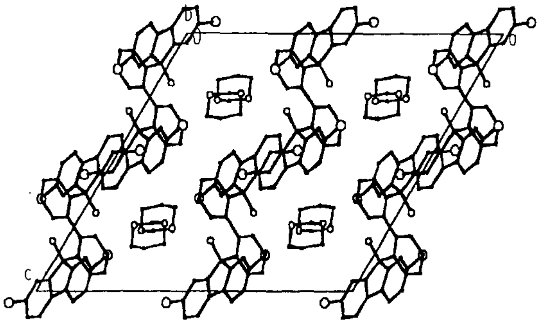

FIGURE 2 Projection of the crystal packing in Compound 2, viewed down [010].

molecules, propagated by a two-fold screw axis, are located in these channels. In each structure the guest molecules are located in the channel with one O atom nearly collinear with the host hydroxyl group, resulting in an intermolecular H-bond which stabilises the structure.

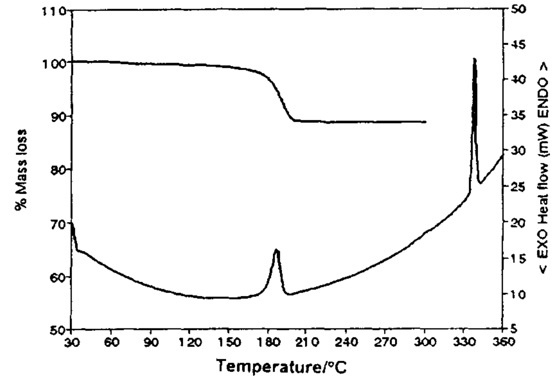

FIGURE 3 Thermal Analysis traces for Compound 1.

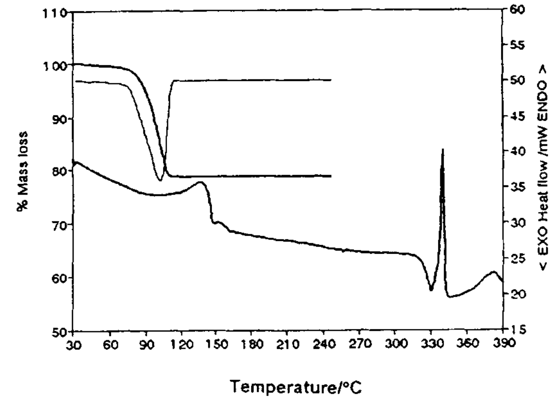

FIGURE 4 Thermal Analysis traces for Compound 2.

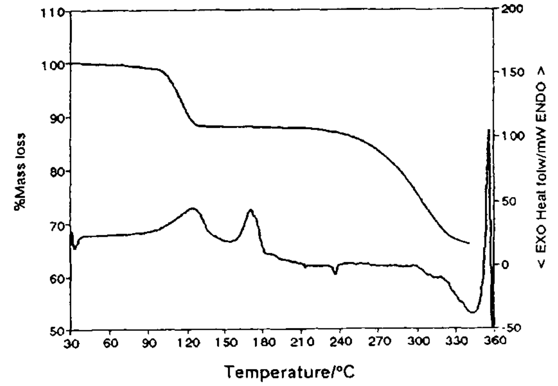

FIGURE 5 Thermal Analysis traces for Compound 3.

Thermal Analysis

The thermal analytical results for Compound **1** are shown in Figure 3. A single mass loss step of 10.8% was observed and corresponds to the loss of one mole of 1,4-dioxane (calc. 10.7%), confirming a host : guest ratio of 1 : 1. The guest loss corresponds to a single endotherm in the DSC trace, with an onset temperature of 179°C. A sharp endotherm, corresponding to the melt of the host compound was observed at 334°C. In Figure 4 the thermal analytical traces for the desolvation of Compound **2** show a single desolvation step of 20.8% mass loss which confirmed the host : guest ratio of 1 : 2 (calc. 21.3%). This corresponded to an endotherm with an onset temperature of 130°C, in the DSC curve. For Compound **3** a single mass loss step in the TG trace corresponds to the guest loss reaction (see Fig. 5), giving rise to an endotherm in the DSC trace, with an onset temperature of 103°C. A second endotherm was observed at 166°C and was attributed to the partial decomposition of the host compound, which gave rise to the discoloration of the host, from a white to a slightly brown powder. A sharp endotherm, corresponding to the melt of the host compound was observed at 357°C.

Kinetics of Desolvation

A series of isothermal TG experiments were carried out on Compound **1**, at 2–3°C intervals over a temperature range of 148–160°C. The resultant mass loss *vs.* time curves were reduced to extent of reaction (α) *vs.* time curves. These curves were deceleratory and the data were best fitted over an α range of 0.05–0.95 by the first order (F1) reaction mechanism $kt = -\ln(1-\alpha)$. A plot of $\ln k$ *vs.* $1/T$ is shown in Figure 6, and yielded an activation energy of 150(6) kJ/mol.

The programmed temperature TG runs obtained for Compounds **2** and **3** were analysed according to a method described by Borchardt and Daniels [12] in order to obtain kinetic parameters. The mass loss *vs.* temperature curves were converted to α *vs.* time curves, since $\alpha = (\text{mass}_t/\text{mass}_{\text{Total}})$, where mass_t is the mass loss at a given time t, $\text{mass}_{\text{Total}}$ is the total mass loss and $t = T/\varphi$, where t is time in seconds, T is temperature in °C and φ is the heating rate in °C/second. An Arrhenius plot can be acquired, if the kinetic model is known, since $g(\alpha) = (1/k)(d\alpha/dt)$. A variety of kinetic models [6] were tested for linearity, and the first order reaction mechanism (F1) gave the best fit of the data for Compound **3**. It yielded an activation energy of 136(5) kJ·mol^{-1} for the desolvation reaction, over an α-range of 0.25–0.90. For the desolvation of Compound **2** the two dimensional growth model (R2), $kt = 1-(1-\alpha)^{1/2}$ fitted the data over an α-range of 0.03–0.99. The semilogarithmic plot yielded an activation energy of 122(2) kJ·mol^{-1}.

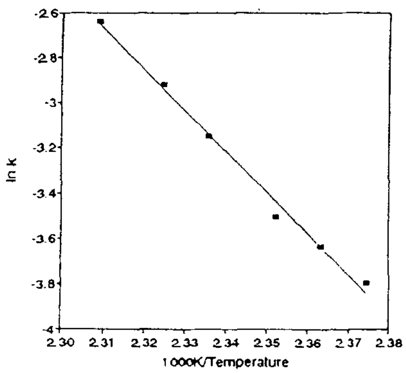

FIGURE 6 Arrhenius plot for the desolvation of Compound **1**.

In Compound **1**, the host structure is stabilised *via* an intramolecular hydrogen bond and the 1,4-dioxane guest molecules are in turn hydrogen bonded to the host compound. The guest molecules are located in constricted channels. Compound **2** and Compound **3** exhibit similar crystal packing and hydrogen bonding motifs. In each case the guest molecules are located in channels running parallel to [010] and are hydrogen bonded to the host *via* one hydrogen bond.

The desolvation of all the inclusion compounds under investigation in this study followed deceleratory kinetic models. In Table II the kinetic parameters and inclusion modes of various inclusion compounds are compared. It is clear from this comparison that the desolvation of Compound **1** requires a higher activation energy than any of the compounds in which the guests are located in channels.

X-Ray Powder Diffraction

X-ray powder diffraction data were collected for the inclusion compounds as well as the desolvation products in each case. It was found that desolvation is always accompanied by a phase change. The host framework collapses to the non-porous alpha-phase of the host alone upon guest loss.

TABLE II

Compound	Kinetic model	$E_a/\text{kJ·mol}^{-1}$	ln A	Inclusion mode
1	F1	150(6)	35.05	Constricted Channel
2	R2	122(2)	44.13	Channel
3	F1	136(5)	38.98	Channel
4 [2]	F1	34(3)	4.32	Channel
4 [2]	F1	111(9)	22.6	Channel
5 [2]	R2	129(16)	35.81	Channel

CONCLUSION

Hydrogen bonds were formed between the host hydroxyl groups and the guest compounds. From the crystal structure solutions it was evident that the guest molecules in these structures were either located in channels (Compounds **2** and **3**) or in constricted channels (Compound **1**).

The kinetics of desorption of similar host-guest inclusion compounds were compared in this study. The activation energies, obtained for these reactions ranged from 35 to 150 $\mathrm{kJ \cdot mol^{-1}}$. Host-guest desolvation reactions show relatively low activation energies, compared with the decomposition of inorganic salts [13]. This is not surprising, since guest desolvation does not require the breaking of covalent bonds, but at most the dissociation of hydrogen bonds. The α *versus* time curves for the desolvation of all the compounds are deceleratory. The loss of the guest is accompanied by a phase change from the host : guest β-phase to the non-porous host α-phase. The constricted channel structure observed for Compound **1** would imply that the gaseous decomposition product cannot escape readily. The inclusion compound is stabilised by additional hydrogen bonding. The host intramolecular hydrogen bond observed in Compound **1** is absent in the other structures. It is important to note that the phase change which accompanies the guest loss reaction in each case cannot be accounted for in the kinetic models, since the extent of reaction was measured as a function of mass loss. It is not possible to postulate complete reaction mechanisms for these reactions without knowing the crystal structures of the resultant α-phases.

Acknowledgements

E. W. thanks the Deutsche Forschungsgemeinschaft and the Fonds der Chemischen Industrie and M.R.C, A.C. and L.R.N. thank the Foundation for Research Development and the University of Cape Town for financial support.

References

[1] Csöregh, I., Weber, E., Nassimbeni, L. R., Gallardo, O. and Dörpinghaus, N. (1993). *J. Chem. Soc. Perkin Trans. 2*, p. 1775.

[2] Weber, E. (1996). *Comprehensive Supramolecular Chemistry*, Vol. 6, Eds. MacNicol, D. D., Toda, F. and Bishop, R., Elsevier, Oxford, p. 535.

[3] Weber, E., Wierig, A. and Scobridis, K. (1996). *J. Prkt. Chem.*, **338**, 553.

[4] Barbour, L. J., Bourne, S. A., Caira, M. R., Nassimbeni, L. R., Weber, E. and Wierig, A. (1993). *Supramolecular Chem.*, **1**, 331.

[5] Bourne, S. A., Nassimbeni, L. R., Niven, M. L., Weber, E. and Wierig, A. (1994). *J. Chem. Soc. Perkin Trans. 2*, p. 1215.

[6] Brown, M. E., Dollimore, D. and Galwey, A. K. (1980). *Comprehensive Chemical Kinetics*, Eds. Bamford, C. H. and Tipper, C. J., Elsevier, Amsterdam, **22**, 220.

[7] Caira, M. R., Coetzee, A., Nassimbeni, L. R., Weber, E. and Wierig, A. (1995). *J. Chem. Soc. Perkin Trans. 2*, p. 281.

[8] Caira, M. R., Coetzee, A., Nassimbeni, L. R., Weber, E. and Wierig, A. (1997). *J. Chem. Soc. Perkin Trans. 2*, p. 237.

[9] North, A. C. T., Phillips, D. C. and Mathews, F. S. (1968). *Acta Crystallogr.*, **A24**, 351.

[10] Sheldrick, G. M. (1985). SHELX-86, *Crystallographic Computing 3*, Eds. Sheldrick, G. M., Kruger, C. and Goddard, R., Oxford University Press.

[11] Sheldrick, G. M. SHELXL-93: Programme for Crystal Structure Determination, unpublished work.

[12] Borchardt, H. J. and Daniels, F. (1957). *J. Am. Chem. Soc.*, **79**, 41.

[13] Galwey, A. K. (1994). *J. Therm. Anal.*, **41**, 267.